JOURNAL OF COMPUTATIONAL PHYSICS 35, 183–205 (1980)

# A Vortex Method for Blood Flow through Heart Valves

M. F. McCracken

*Department of Mathematics, Indiana University, Bloomington, Indiana 47405*

AND

C. S. Peskin

*Courant Institute of Mathematical Sciences,*
*New York University, New York, New York 10003*

Received January 12, 1979; revised May 18, 1979

A combination vortex–grid method for solving the two-dimensional, incompressible Navier–Stokes equations in regions with complicated internal, elastic boundaries is presented. The authors believe the method to be applicable to the case of at least moderately high Reynolds number flow. The method is applied to the study of blood flow through the mammalian mitral valve. Previous work of Peskin is extended and the conjecture that the behavior of mammalian heart valves is independent of Reynolds number is supported.



## I. Introduction

The purpose of this work is twofold—to develop a numerical method for studying high-Reynolds-number fluid flow in a two-dimensional region with boundaries that may move, and to apply this method to the problem of blood flow through heart valves. In particular, we wished to check the conjecture that mammalian mitral valces behave independently of the Reynolds number: that is, the hearts of different-sized mammals behave like scale models of each other despite variations in the Reynolds numbers over a range of two orders of magnitude (see Kalmanson [5]). Peskin [8] has made a numerical study of blood flow through the mitral valve; however, because of the necessity of refining the mesh, his method could not feasibly be used at Reynolds numbers as high as those of the human heart. The highest Reynolds numbers he could study were about 100 times smaller than those in the range of human physiology. Therefore, before undertaking this work, it was necessary to develop a high-Reynolds-



0021-9991/80/050183-23$02.00/0

number method for solving the incompressible Navier–Stokes equations in the presence of moving, immersed elastic boundaries, the motions of which are not known in advance. Because the geometry of this problem is very complicated, we needed an extremely general method. The best high-Reynolds-number method available for incompressible flow is Chorin's vortex method [1]. This method is grid free and the effects of the boundary on the fluid are realized by having the boundary at each timestep shed point vortices into the fluid. Each vortex then interacts with all the others. Chorin's method is perfectly suited to exterior problems of flow-past-a-body type, because in such cases, the point vortices are swept downstream away from the body, whereupon they may be discarded from the calculation. In other types of problems, however. the method can be prohibitively expensive because the number of vortices grows linearly with time and the number of computations grows quadratically. Shestakov [9] has a hybrid method, involving both point vortices and a mesh which does not have to be refined as the Reynolds number increases. In Shestakov's method, the fluid domain is divided into two parts: a strip of width $\delta$ in the neighborhood of the boundary on which Chorin's vortex method is used and an interior grid on which finite-difference methods are used. The mesh does not have to be refined as the Reynolds number increases because the use of vortices in the boundary layer provides high resolution there. Shestakov's method is therefore especially well suited to a problem with fixed, flat boundaries. In the heart valve problem, the boundary consists of the valve and the heart wall. It is immersed in the fluid, exerts forces on it, and moves at local fluid velocity. We idealize the boundary and assume it to be thin and massless. Thus, a new treatment, applicable to the case of interior, complicated, moving elastic boundaries was necessary.

The case of elastic boundaries creates an additional problem in the use of any vortex method: The creation of vorticity at the boundary now depends on the curl of the (singular) field of boundary forces. Since the boundary points move like fluid markers and their motion is not known in advance, Chorin's algorithm (based on the slip velocity generated during one time step of the Euler equations) for the creation of vorticity cannot be used. Instead, we find that the tangential boundary force acting on the fluid for one time step creates a vortex dipole layer along the boundary and that the derivative of the normal force creates a simple vortex layer. A preliminary test of this approach, in which the boundary forces are used to generate vorticity, appears in the work of Mendez [6], who computed the large-amplitude motion of an elastic ellipse immersed in an inviscid fluid (Euler equations).

A new method, described below, which we believe to be good for solving the two-dimensional Navier–Stokes equations at high Reynolds number has been developed. We emphasize that this method can be used in applications other than blood flow through heart valves. The method can be applied to incompressible flow in a two-dimensional region with thin, massless boundaries which either do not move at all, move in a prescribed manner, or which exert forces on the fluid and move at the local fluid velocity. Note, however, that the same equations of fluid must hold on either side of the boundary. In the former two cases, the method is somewhat simpler than it is in the present example. The only restriction on use of our method is that one must

be able to embed the domain of interest in a larger domain for which a fast Laplace solver is available (e.g., a periodic box) without doing violance to the physics of the problem.[1] Like Shestakov's method, ours combines point vortices and a mesh. The special new features of our method are the generation of point vortices using the boundary forces and the fact that the vortices are retained as such only for a fixed number of timesteps, after which their vorticity is spread to the mesh. A point vortex should be retained for enough timesteps so that it will probably have diffused out of the boundary layer before it is spread to the mesh. Because the boundary layer becomes thinner as the Reynolds number increases, the required number of timesteps does not grow. Preliminary work on our method appears in McCracken and Peskin [11].

Briefly, our method is as follows: the domain on which the fluid flows is the unit square in $R^2$ with periodic boundary conditions. Inside the domain there are moving, elastic boundaries which are assumed to be infinitely thin and massless, and which exert forces on the fluid. These boundaries consist of the heart walls and valve in the case of blood flow.

We use both a Lagrangian representation of the boundary and an Eulerian representation of the fluid on a computational mesh. The boundary is discretized and the positions of the boundary points are stored. The boundary points are not required to fall on mesh points. At each timestep the effects of the boundary forces on the fluid are realized by having the boundary shed point vortices into the fluid. There are several ways to do this: they will be reviewed in Section IV. The positions and strengths of the point vortices are stored for a certain fixed number of timesteps, after which their vorticity is spread to the mesh and they are discarded as point vortices. The effect of this is that the number of point vortices does not grow with time. At any time the total vorticity is the sum of the vorticity due to the point vortices and that on the mesh.

The procedure at each timestep is first to update the boundary forces. Next the vorticity of the oldest point vortices is spread to the mesh and new vortices are created in their stead, using the boundary forces. The mesh vorticity is then updated using a finite-difference form of the vorticity transport equation. The velocity field is found by differencing the stream function, which is computed from the total vorticity by means of a fast Laplace solver. On a fixed mesh, the number of operations in the computation of the velocity by this method grows only linearly with the number of vortices. Finally, the boundary points and vortices are moved in the velocity field by interpolating the velocity from the mesh. The vortices are also walked one random step because of viscous diffusion.

Note that the vortices affect each other through the mesh, that is, the velocity one point vortex produces at another is not computed directly. This is done to save computing time. At very high Reynolds number it would be desirable to have a local correction to this so that the velocity at a point vortex due to nearby vortices would, in effect, be computed directly.

[1] A referee has pointed out that a fast Laplace solver is not strictly necessary, since one can solve the stream function equation by iterative methods using the previous time step as an initial guess. However, in that case, the method would be slower to execute than it is when a fast solver is used.

It should now be pointed out that an objection to our method can be raised exactly because we move the vortices through the mesh. This objection as especially well put by one of the referees, who said, "Much filtering is going on when the vortices and normal forces are spread to the mesh and when the velocities are interpolated back onto the vortices and boundaries. Scales of motion smaller than the mesh width, $h$, will not be properly represented by these procedures. These scales are assumed to exist, otherwise the hybrid scheme would not be necessary. Even the procedure of placing the dipole point vortices on the boundaries a distance $h$ apart is mesh dependent rather than Re dependent..." As these remarks indicate, the statements in this paper concerning the effects of Reynolds number should be read as conjectures and not as established facts. Further numerical experiments will be required to determine the range of Reynolds numbers that is appropriate for vortex–grid methods (see also [10]).

## II. Equations of Motion

In nondimensional form, the equations of motion for incompressible flow are as follows:

$$\begin{aligned} \frac{\partial \mathbf{u}}{\partial t} + \mathbf{u} \cdot \nabla \mathbf{u} + \nabla p &= \frac{1}{R} \Delta \mathbf{u} + \mathbf{F}, \\ \nabla \cdot \mathbf{u} &= 0, \end{aligned} \tag{2.1}$$

where $\mathbf{u}$ is the fluid velocity, $p$ is the pressure, $R$ is the Reynolds number, and $\mathbf{F}$ is the boundary force. Further, we have

$$\frac{\partial \mathbf{X}}{\partial t} = \mathbf{u}(\mathbf{X}(s, t), t), \tag{2.2}$$

where $\mathbf{X}(s, t)$ is the Lagrangian representation of the boundary, that is, fixed $s$ marks a material point and, for fixed $t$, $\mathbf{X}(\cdot, t)$ is a parametrization of the boundary. $A$ (below) is assumed to be constant in time, so it may be taken to be length of the boundary at time $t = 0$, for example. Finally,

$$\mathbf{F}(\mathbf{x}, t) = \int_0^A \mathbf{f}(x, t)\, \delta(\mathbf{x} - \mathbf{X}(s, t))\, ds, \tag{2.3}$$

where $\delta$ is the two-dimensional Dirac $\delta$-function and $\mathbf{f}$ is the force density, which can be computed from the boundary configuration $\mathbf{X}$. Note that since $\mathbf{X}$ is a curve, i.e., one-dimensional, for each fixed $t$, and $\delta$ is the two-dimensional $\delta$-function, $\mathbf{F}(\mathbf{x}, t)$ is singular.

Taking the curl of the first equation and letting $\omega \hat{\mathbf{z}} = \nabla \times \mathbf{u}$, where $\hat{\mathbf{z}}$ is a unit vector perpendicular to the plane of the flow, we get,

$$\frac{\partial \omega}{\partial t} + \nabla \cdot (\mathbf{u}\omega) = \frac{1}{R} \Delta \omega + \hat{\mathbf{z}} \cdot (\nabla \times \mathbf{F}), \tag{2.4}$$

which is the vorticity transport equation. In the particular example we are considering, we do not have $\nabla \cdot (\mathbf{u}\omega) = \mathbf{u} \cdot \nabla\omega$ everywhere because there is a point source of volume in the atrium of the heart (see Section VII). It can be seen from this equation that $\nabla \times F$ generates vorticity in the fluid. In our case, the support of $\mathbf{F}$ is the boundary, and we inject vorticity into the boundary layer using a formula derived by taking thr curl of the singular boundary forces (see Section III).

Although the method of this paper is designed for incompressible flow, it can also accomodate the situation in which the domain contains sources and sinks so that $\nabla \cdot \mathbf{u} \neq 0$. It follows that $\nabla \cdot (\mathbf{u}\omega)$ cannot be replaced by $\mathbf{u} \cdot \nabla\omega$. The form $\nabla \cdot (\mathbf{u}\omega)$ has certain numerical advantages in any case, as we explain in Section VII. In the presence of sources and sinks, the equations that determine the convection velocity $\mathbf{u}$ become $\nabla \times \mathbf{u} = \omega\hat{\mathbf{z}}$ and $\nabla \cdot \mathbf{u} = \sigma$, where $\sigma$ is the (given) source distribution. We can write $\mathbf{u} = \mathbf{u}_\omega + \mathbf{u}_\sigma$, where

$$\nabla \times \mathbf{u}_\omega = \omega\hat{\mathbf{z}}, \qquad \nabla \cdot \mathbf{u}_\omega = 0,$$
$$\nabla \times \mathbf{u}_\sigma = 0, \qquad \nabla \cdot \mathbf{u}_\sigma = \sigma.$$

Thus the sources contribute a potential flow which is independent of the distribution of vorticity.

In our application, we have a source in the left atrium and a sink around the edges of the domain. The source corresponds to the pulmonary veins, and the sink accomodates the volume displaced by the moving walls of the heart. (The strength of the sink is determined by that of the source, since volume is conserved.) A similar technique was used in Peskin [8], but here we take the strength of the source as constant, while in [8] the source was pressure-dependent. It would be difficult to use a pressure-dependent source in the present context, since the pressure is not computed. It would be very easy, however, to make the source strength a given function of time.

One always computes the boundary forces from the boundary configuration. This is rather complicated in the case of elastic boundaries and will be detailed in Section IV. However, if the boundary does not move or moves in a prescribed manner, it is a simple matter to compute the forces. In that case, the force at each boundary point depends only on that boundary point and not on any of the other ones. Each boundary point should be attracted to its equilibrium position, or the position prescribed by the boundary motion, with a force depending only on how far the point is from where it should be. The force should be sufficiently large to keep the boundary point very close to the right place, but not so large as to cause instability.[2]

## III. Generation of Vortices Using the Boundary Forces

The key to the numerical method presented in this paper is the way in which the boundary forces are used to shed point vortices into the fluid, because it is these

[2] In other words, we may take $\mathbf{F}(\mathbf{x}, t) = \mathbf{C}[\mathbf{x} - \mathbf{x}_e(t)]$, where $\mathbf{x}_e(t)$ is the desired configuration of the boundary at time $t$.

vortices which make it possible to study high-Reynolds-number flow without refining the mesh. Vortices may be shed in vortex dipole pairs or in dipole pairs together with single vortices.

To understand what a point vortex is, imagine stationary, incompressible flow in which $\omega(\mathbf{x}) = K\delta(\mathbf{x} - \mathbf{x}_0)$. Recall that there will be a stream function $\psi(\mathbf{x})$ such that if $\mathbf{u}(\mathbf{x}) = (u_1(\mathbf{x}), u_2(\mathbf{x}))$ is the velocity field, then $\partial\psi/\partial x_2 = -u_1$ and $\partial\psi/\partial x_1 = u_2$. Hence, we obtain $\Delta\psi(\mathbf{x}) = \omega(\mathbf{x}) = K\delta(\mathbf{x} - \mathbf{x}_0)$. Solving this, we aesily see that

$$\mathbf{u}(\mathbf{x}) = \frac{\hat{\mathbf{z}} \times (\mathbf{x} - \mathbf{x}_0)K}{|\mathbf{x} - \mathbf{x}_0|^2 2\pi}. \tag{3.1}$$

Thus, the velocity field due to a point vortex has circular streamlines and the magnitude of the velocity falls off as $1/|\mathbf{x} - \mathbf{x}_0|$. The circulation around any simple, closed curve is $K$ if $\mathbf{x}_0$ is in the interior of the curve and zero otherwise. By a vortex dipole we shall mean a pair of point vortices with equal but opposite strengths. If the positive and negative vortices of the dipole are at points $\mathbf{x}$ and $\mathbf{y}$, respectively, then $(\mathbf{x} - \mathbf{y})K$ is the vortex dipole moment of the pair.

We now make the argument which shows how point vortices are generated by the forces. Below, for convenience we suppress dependence on time. If $\mathbf{F}$ is the force, then

$$\mathbf{F}(\mathbf{x}) = \int_0^A \mathbf{f}(s)\,\delta(\mathbf{x} - \mathbf{X}(s))\,ds, \tag{3.2}$$

so that

$$\begin{aligned}(\nabla \times \mathbf{F}) \cdot \hat{z} &= \int_0^A \{\nabla \times [\delta(\mathbf{x} - \mathbf{X}(s))\,\mathbf{f}(s)]\} \cdot \hat{\mathbf{z}}\,ds \\ &= \int_0^A \nabla \cdot \{\delta(\mathbf{x} - \mathbf{X}(s))\,\mathbf{f}(s) \times \hat{\mathbf{z}}\}\,ds \\ &= \int_0^A \nabla\delta(\mathbf{x} - \mathbf{X}(s)) \cdot \{\mathbf{f}(s) \times \hat{\mathbf{z}}\}\,ds.^3\end{aligned} \tag{3.3}$$

Taking the dipole moment of this expression over an arbitrary region $R_1$ of fluid, we get that it is equal to $\int_{R_1 \cap \mathbf{X}} (-f_2(s), f_1(s))\,ds$. Thus, $(-f_2(s), f_1(s))$ is the dipole moment density along the boundary. It is natural to discretize this as a layer of vortex dipoles. Note that they are not necessarily oriented normally to the boundary. Adopting this point of view, when the boundary is discretized, at each boundary point, at each timestep, a vortex dipole pair as above is shed into the fluid.

A more refined viewpoint leads to a more natural discretization, and, judging by the results, to greater numerical stability. We separate the forces into components tangent and normal to the boundary. Let $\mathbf{f}(s) = f_\tau\boldsymbol{\tau} + f_n\mathbf{n}$, where $\boldsymbol{\tau}$ and $\mathbf{n}$ are unit

[3] Note that differentiation is with respect to $\mathbf{x}$ only. Thus, $\mathbf{f}(s)$, $\mathbf{X}(s)$, $\hat{\mathbf{z}}$ all function as constants.

vectors parallel and perpendicular, respectively, to the boundary. Then $\mathbf{f}(s) \times \hat{\mathbf{z}} = f_n\boldsymbol{\tau} - f_\tau\mathbf{n}$ and so,

$$(\nabla \times \mathbf{F}) \cdot \hat{\mathbf{z}} = \int_0^A \{\nabla\delta(\mathbf{x} - \mathbf{X}(s))\} \cdot f_n\boldsymbol{\tau}\, ds - \int_0^A \{\nabla\delta(\mathbf{x} - \mathbf{X}(s))\} \cdot f_\tau\mathbf{n}\, ds. \quad (3.4)$$

Consider the first term,

$$\int_0^A \{\nabla\delta(\mathbf{x} - \mathbf{X}(s))\} f_n\boldsymbol{\tau}\, ds. \quad (3.5)$$

We have that

$$\nabla\delta(\mathbf{x} - \mathbf{X}(s)) \cdot \boldsymbol{\tau}(s) = \frac{-1}{|\mathbf{X}'(s)|} \frac{d\delta(\mathbf{x} - \mathbf{X}(s))}{ds}, \quad \text{where} \quad |X'(s)| = (X_1'(s)^2 + X_2'(s)^2)^{1/2}. \quad (3.6)$$

Integrating by parts, we obtain

$$\begin{aligned} &\int_0^A \{\nabla\delta(\mathbf{x} - \mathbf{X}(s))\} \cdot f_n(s)\,\boldsymbol{\tau}(s)\, ds \\ &\quad = -\frac{\delta(\mathbf{x} - \mathbf{X}(s))\, f(s)}{|\mathbf{X}'(s)|}\Bigg|_0^A + \int_0^A \frac{d}{ds}\left(\frac{f_n(s)}{|\mathbf{X}'(s)|}\right)\delta(\mathbf{x} - \mathbf{X}(s))\, ds \\ &\quad = \int_0^A \frac{d}{ds}\left(\frac{f_n(s)}{|\mathbf{X}'(s)|}\right)\delta(\mathbf{x} - \mathbf{X}(s))\, ds, \end{aligned} \quad (3.7)$$

in the case where the boundary is a simple closed curve. The integral has the natural interpretation of being a $\delta$-layer of vorticity with strength density

$$\frac{d}{ds}\left(\frac{f_n(s)}{|\mathbf{X}'(s)|}\right)$$

along the boundary. This point of view leads, upon discretization, to having the normal forces shed single vortices into the fluid and the tangential forces shed dipoles, which would now be oriented normally to the boundary.

Once the normal and tangential forces have been separated, several variants of the method are possible. One can, for example, use the normal forces to create vorticity directly on the mesh and use only the tangential forces in the creation of point vortices in the form of vortex dipoles. This is what we have done because of our belief that the tangential forces have the greater influence on the boundary layer at high Reynolds number. The other possibilities are currently being checked in the work in progress mentioned in the Introduction.

## IV. The Heart and Its Boundary Forces

The setup of the heart and its muscular links is the same here as in Peskin [8]. We, therefore, refer the reader to that paper for details is and merely provide a sketch here.

Further background on mitral valve dynamics and on related aspects of cardiac physiology may be found in [5, 7].

We wish to study blood flow through the mitral valve, which is the inflow valve of the left ventricle. Blood returning from the lungs to the heart enters the left atrium, from which it is transferred to the left ventricle across the mitral valve. In order to study the flow patterns of the mitral valve, we need to construct a representation of the heart which includes at least the left atrium and ventricle. We study only the filling cycle, so we do not need the aortic valve. However, we do need the outflow tract because its geometry is important in the performance of the mitral valve. The heart is constructed from musculat and elastic links, as described below, arranged in the two-dimensional geometry as shown in Fig. 1. This arrangement resembles a cross

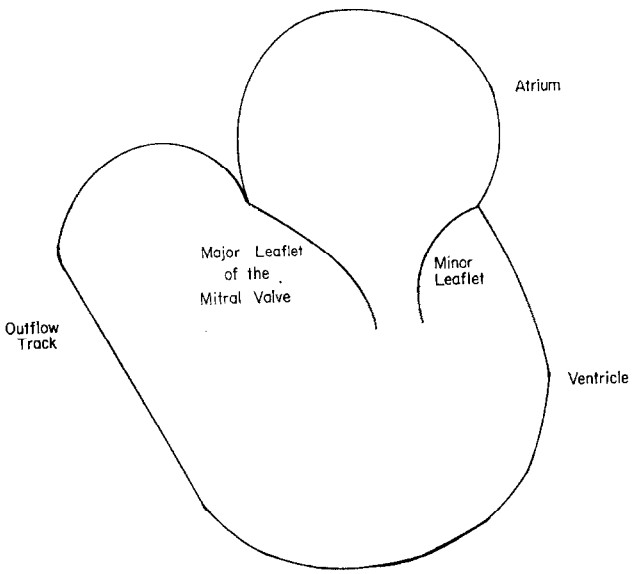


FIG. 1. The two-dimensional geometry used in the computation.

section of the left heart in a plane which bisects the two major leaflets of the mitral valve and which also passes through the apex of the heart. The physical quantities which set the scale for the fluid dynamics of the human mitral valve are

$$\begin{aligned} L_0 &= 3.2 \text{ cm} = \text{diameter of mitral ring,} \\ T_0 &= 0.86 \text{ sec} = \text{duration of a heartbeat} \\ \nu &= 0.04 \text{ cm}^2/\text{sec} = \text{viscosity.} \end{aligned} \tag{4.1}$$

These can be combined to give the Reynolds number $R = L_0^2/\nu T_0 \cong 300$. It is very important to note that this definition of Reynolds number is rather arbitrary. For example, it would perhaps be better to take as the characteristic time the duration of

the rapid filling phase of diastole which is about $T_0/4$, which results in a Reynolds number of 1200 for the human heart (a more standard figure). Any such definition will work, and different choices of the reference length and of the reference time will simply result in a different (but equivalent) system of nondimensional variables.

It seems reasonable to treat the valve leaflet and heart wall as immersed boundaries in the fluid because these parts of the heart are, in fact, incompressible and neutrally buoyant in blood. Because most of the action takes place inside the heart, the requirement that the heart be embedded in a periodic box should not interfere with valve performance.

We now briefly describe how the boundary forces are derived from the boundary configuration. The boundary is discretized into finitely many points $\{\mathbf{X}_n\}_{n=1}^{n=N}$. The force density at each point $\mathbf{X}_k$ is a function $\mathbf{f}_k(\mathbf{X}_1, \ldots, \mathbf{X}_N)$. We now restrict the form of these functions by assuming that the forces arise in straight-line segments (links) connecting specified pairs of boundary points. Suppose that link $kj$ connects $\mathbf{X}_j$ and $\mathbf{X}_k$, and let

$$\begin{aligned} \mathbf{X}_{jk} &= \mathbf{X}_j - \mathbf{X}_k, \\ L_{jk} &= |\mathbf{X}_{jk}|, \\ T_{jk}(L_{jk}) &= \text{tension in link } jk; \end{aligned} \tag{4.2}$$

then

$$\frac{1}{N}\mathbf{f}_j = \sum_{\substack{k=1 \\ j \neq k}}^{N} T_{jk}\frac{\mathbf{X}_{jk}}{L_{jk}}. \tag{4.3}$$

In the present calculation, each link has a length tension relation

$$\begin{aligned} T_{jk}(L_{jk}) &= (L_{jk} - L_{jk}^{\circ})\, S_{jk}, \qquad L_{jk} > L_{jk}^{\circ}, \\ &= 0, \qquad\qquad\qquad L_{jk} \leqslant L_{jk}^{\circ}, \end{aligned} \tag{4.4}$$

where $S_{jk}$ is the stiffness and $L_{jk}^{\circ}$ the resting length.

It should be emphasized that the heart valve problem is very sensitive to the treatment of the boundary. Thus, in updating the forces, an implicit scheme must be used for numerical stability. In the process, an equation of the form

$$\mathbf{X}_k^* = \mathbf{X}_k + \lambda \mathbf{f}_k(\mathbf{X}_1^*, \ldots, \mathbf{X}_N^*) \tag{4.5}$$

must be solved. The derivation of this equation and its solution by Newton's method are discussed in Peskin [8]. It is proved there that the matrix which arises in this application of Newton's method is symmetric and positive definitive whenever the tension in each link satisfies $T(L) \geqslant 0$, $T'(L) \geqslant 0$.

## V. Chorin's Vortex Method

The numerical method for solving the Navier–Stokes equations that we present in this paper is a hybrid of Chorin's vortex method [1], which uses modified point

vortices only, and a finite-difference method using a mesh. In the following two sections we briefly describe both methods. For the sake of simplicity, we describe them in the case where there are no boundaries and no external forces.

To solve an initial value problem by Chorin's vortex method, one first divides the region up into boxes and places a point vortex at the center of each box. The strength $K_j$ of the $j$th vortex should be the integral of $\omega^0$, the initial vorticity, over the box. Once this is done, we forget all about the boxes. The vortices move according to convection and diffusion. The velocity due to Chorin's vortices is the same as that given in Section III except that it is modified to smooth out the singularity at the vortex. Thus the velocity $\mathbf{u}_k$ generated by the $k$th vortex is defined to be

$$\begin{aligned} \mathbf{u}_k(x) &= \frac{\hat{\mathbf{z}} \times (\mathbf{x} - \mathbf{x}_k) K_k}{2\pi \mid \mathbf{x} - \mathbf{x}_k \mid^2} \qquad \text{if} \quad \mid \mathbf{x} - \mathbf{x}_k \mid > d \\ &= \frac{\hat{\mathbf{z}} \times (\mathbf{x} - \mathbf{x}_k) K_k}{2\pi \mid \mathbf{x} - \mathbf{x}_k \mid d} \qquad \text{if} \quad \mid \mathbf{x} - \mathbf{x}_k \mid < d. \end{aligned} \tag{5.1}$$

Note that the speed is constant inside the circle of radius $d$ about $\mathbf{x}_k$. The use of this particular smoothing is motivated by considerations involving the no-slip condition in the bounded case. Although these considerations are inapplicable in our problem, some smoothing is necessary. This smoothing is automatically accomplished in our hybrid method because the vortices are moved through the mesh (see Section VII). Chorin's algorithm for moving the vortices at each timestep $\Delta t$ is

$$\mathbf{x}_j^{n+1} = \mathbf{x}_j^n + \Delta t \sum_{k \neq j} \mathbf{u}_k^n(\mathbf{x}_j) + \hat{\eta}_j^n, \tag{5.2}$$

where the superscript $n$ refers to the $n$th timestep, and $\mathbf{u}_k^n$ is the velocity field induced by the $k$th vortex at the $n$th timestep. The last term, $\eta_j^n$, is a random step, representing diffusion. The $\eta_j$v's are independent, Gaussian random variables with expectation equal to zero and variance equal to $\Delta t/R$. The scheme can be modified to handle the case of bounded domains. If one leaves out the random walk, the scheme can be used to solve Euler's equations and it is known to converge (see Dushane [2] and Hald [4]).

## VI. The Timesplitting Difference Scheme

The finite-difference part of our numerical method is based on a timesplitting difference scheme. This scheme is very similar to the scheme used by Shestakov [9]; the two schemes differ only in their treatment of the inertial terms in the Navier–Stokes equations. Let the domain be periodic and have no internal boundaries. For the purposes of this section, assume the force $\mathbf{F}$ is given. The equations may be written

$$\begin{aligned} \frac{\partial \omega}{\partial t} + \nabla \cdot (\mathbf{u}\omega) &= \frac{1}{R}\Delta\omega + \nabla \times \mathbf{F}, \\ \Delta\psi &= \omega, \\ u_1 &= -\frac{\partial \psi}{\partial x_2}, \\ u_2 &= \frac{\partial \psi}{\partial x_1}. \end{aligned} \tag{6.1}$$

Let $D_{\pm 1}$ and $D_{\pm 2}$ be the forward and backward divided difference operators in $x_1$ and $x_2$, respectively, e.g.,

$$(D_{-1}\phi)_{ij} = \frac{\phi_{ij} - \phi_{i-1j}}{h}, \tag{6.2}$$

where $h$ is the mesh width and $ij$ refers to the mesh point at $(ih, jh)$. Let $D_{01}$ and $D_{02}$ be the centered divided differences, e.g.,

$$D_{01} = \frac{1}{2h}(D_{+1} + D_{-1}), \tag{6.3}$$

and lastly let $C\mathbf{u}$ be the discrete curl,

$$(C\mathbf{u})_{ij} = D_{01}u_2 - D_{02}u_1 . \tag{6.4}$$

In the timesplitting scheme an intermediate vorticity field is calculated. The scheme is

$$\begin{aligned} \omega^{n+1/2} - \omega^n = \frac{\Delta t}{2}\Big(&-D_{01}(u_1{}^n\omega^{n+1/2}) - D_{02}(u_2{}^n\omega^n) + \frac{1}{R}D_{+1}D_{-1}\omega^{n+1/2} \\ &+ \frac{1}{R}D_{+2}D_{-2}\omega^n + C\mathbf{F}^{n+1}\Big), \end{aligned} \tag{6.5}$$

$$\begin{aligned} \omega^{n+1} - \omega^{n+1/2} = \frac{\Delta t}{2}\Big(&-D_{01}(u_1{}^n\omega^{n+1/2}) - D_{02}(u_2{}^n\omega^{n+1}) + \frac{1}{R}D_{+1}D_{-1}\omega^{n+1/2} \\ &+ \frac{1}{R}D_{+1}D_{-2}\omega^{n+1} + C\mathbf{F}^{n+1}\Big), \end{aligned} \tag{6.6}$$

$$\begin{aligned} (D_{01}^2 + D_{02}^2)\,\psi^{n+1} &= \omega^{n+1}, \\ -D_{02}\psi^{n+1} &= u_1^{n+1}, \\ D_{01}\psi^{n+1} &= u_2^{n+1}. \end{aligned} \tag{6.7}$$

Note that in (6.5) the $x_1$ differencing is implicit and the $x_2$ differencing explicit and that this is reversed in (6.6).

In Shestakov [9] the scheme used to solve the vorticity transport equation is similar

to (6.5)–(6.6) except that Shestakov uses $-u_1{}^n D_{01}(\omega^{n+1/2})$ instead of $-D_{01}(u_1{}^n\omega^{n+1/2})$ and similarly for all the other nonlinear terms. Our scheme differs in this respect for two reasons. First, because of the point source of volume in the heart we do not have $\nabla \cdot (\mathbf{u}\omega) = \mathbf{u} \cdot \nabla\omega$ everywhere. Second, we need $\sum_{i,j} \omega^{n+1}_{2i+p,2j+q} = 0$ for $p, q \in \{0, 1\}$ because of periodicity (see below). Conservative differencing preserves this property, as we shall see. There is one other difference between the two schemes. Shestakov uses the Laplacian $Dq_1D_{-1} + Dq_2D_{-2}$ in the equation for the stream function $\psi$. A possible advantage in our use of $D^2_{01} + D^2_{02}$ to represent the Laplacian is that we then have exactly $\omega = C\mathbf{u}$.

There is no known convergence proof for either version of this timesplitting scheme; however, in the case of linear, constant coefficients, that is, in the case where $\mathbf{u}$ is a known constant vector, both versions of (6.5)–(6.6) converge. To find $\omega^{n+1}$ one solves tridiagonal matrix systems, which can be done efficiently by factorization. Details of the preceding assertions may be found in Shestakov [9].

After $\omega^{n+1}$ has been found, $\psi^{n+1}$ can be found by using the fast Laplace solver of [3]. Note that, for a square mesh when the number of mesh points is even, solving $(D^2_{01} + D^2_{02})\,\psi = \omega$ is equivalent to solving $(D_{+1}D_{-1} + D_{+2}D_{-2})\,\psi = \omega$ on the four meshes $M_{\omega q} = \{(p + 21), (q + 2j)\}_{i,j}$, where $p, q \in \{0, 1\}$. Because of periodicity, the range of $(D^2_{01} + D^2_{02})$ is the space of all mesh functions $\omega$ which satisfy $\sum_{(i,j)\in M_{pq}} \omega_{ij} = 0$ for each $p, q$. We now show that our version of the timesplitting scheme preserves this property with increasing $n$. Consider

$$\omega^{n+1/2}_{ij} + \frac{\Delta t}{4h}\left(u^n_{1,i+1j}\omega^{n+1/2}_{i+1j} - u^n_{1,i-1j}\omega^{n+1/2}_{i-1j}\right) - \frac{\Delta t}{2Rh^2}\left(\omega^{n+1/2}_{i+1j} + \omega^{n+1/2}_{i-1j} - 2\omega^{n+1/2}_{ij}\right)$$

$$= \omega^n_{ij} - \frac{\Delta t}{4h}\left(u^n_{2,ij+1}\omega^n_{ij+1} - u^n_{2,ij-1}\omega^n_{ij-1}\right)$$

$$+ \frac{\Delta t}{2Rh^2}\left(\omega^n_{ij+1} + \omega^n_{ij-1} - 2\omega^n_{ij}\right) + \frac{\Delta t}{2}\left(C\mathbf{F}^{n+1}\right)_{ij}. \tag{6.8}$$

First note that $\sum_{(i,j)\in M_{pq}} C\mathbf{F}^{n+1}_{ij} = 0$ because

$$\left(C\mathbf{F}^{n+1}\right)_{ij} = \frac{F^{n+1}_{2,i+1j} - F^{n+1}_{2,i-1j}}{2h} + \frac{F^{n+1}_{1,ij-1} - F^{n+1}_{1,ij+1}}{2h} \tag{6.9}$$

and because of the periodicity. We let $S^n_{pq} = \sum_{(i,j)\in M_{pq}} \omega_{ij}$ and sum (6.8) over $M_{00}$ and obtain

$$S^{n+1/2}_{00} - \frac{\Delta t}{2Rh^2}\left(2S^{n+1/2}_{10} - 2S^{n+1/2}_{00}\right) = S^n_{00} + \frac{\Delta t}{2Rh^2}\left(2S^n_{01} - 2S^n_{00}\right) \tag{6.10}$$

and summing over the other three $M_{pq}$'s, we obtain three other, similar equations. Letting $\beta = \Delta t/Rh^2$, $\mathbf{S}^n = (S^n_{00}, S^n_{10}, S^n_{01}, S^n_{11})$, and $A(\beta)$ denote the matrix

$$A(\beta) = \begin{bmatrix} 1 + \beta & -\beta \\ -\beta & 1 + \beta \end{bmatrix}, \tag{6.11}$$

we can write our four equations in block matrix form as

$$\begin{bmatrix} A(\beta) & 0 \\ 0 & A(\beta) \end{bmatrix} \mathbf{S}^{n+1/2} = \begin{bmatrix} (1-\beta)I & \beta I \\ \beta I & (1-\beta)I \end{bmatrix} \mathbf{S}^{n}. \tag{6.12}$$

By an analogous procedure, we obtain

$$\begin{bmatrix} (1+\beta)I & -\beta I \\ -\beta I & (1+\beta)I \end{bmatrix} \mathbf{S}^{n+1} = \begin{bmatrix} A(-\beta) & 0 \\ 0 & A(-\beta) \end{bmatrix} \mathbf{S}^{n+1/2}, \tag{6.13}$$

so that letting

$$\mathscr{A}_\beta = \begin{bmatrix} A(\beta) & 0 \\ 0 & A(\beta) \end{bmatrix} \quad \text{and} \quad \mathscr{B}_\beta = \begin{bmatrix} (1+\beta)I & -\beta I \\ -\beta I & (1+\beta)I \end{bmatrix}$$

we have

$$\mathbf{S}^{n+1} = \mathscr{B}_\beta^{-1}\mathscr{A}_{-\beta}\mathscr{A}_\beta^{-1}\mathscr{B}_{-\beta}\mathbf{S}^n. \tag{6.15}$$

However, since it is clear that $\mathscr{B}_{-\beta}$ commutes with $\mathscr{A}_{-\beta}$ and $\mathscr{A}_\beta$, $\mathscr{B}_{-\beta}$ also commutes with their inverses, so that we see

$$\mathbf{S}^{n+1} = \mathscr{B}_\beta^{-1}\mathscr{B}_{-\beta}\mathscr{A}_{-\beta}\mathscr{A}_\beta^{-1}\mathbf{S}^n. \tag{6.16}$$

Now, it is easily seen that

$$A(-\beta)\,A^{-1}(\beta) = \frac{1}{2\beta+1}\begin{bmatrix} 1 & 2\beta \\ 2\beta & 1 \end{bmatrix}, \tag{6.17}$$

and hence that

$$\mathscr{B}_\beta^{-1}\mathscr{B}_{-\beta} = \frac{1}{(2\beta+1)}\begin{bmatrix} I & 2\beta I \\ 2\beta I & I \end{bmatrix}. \tag{6.18}$$

Multiplying the matrices together, we obtain that

$$\mathbf{S}^{n+1} = \frac{1}{(2\beta+1)^2}\begin{bmatrix} C(\beta) & 2\beta C(\beta) \\ 2\beta C(\beta) & C(\beta) \end{bmatrix} \mathbf{S}^n, \tag{6.19}$$

where

$$C(\beta) = \begin{bmatrix} 1 & 2\beta \\ 2\beta & 1 \end{bmatrix}. \tag{6.20}$$

It is then easily seen that

$$S^{n+1} \leqslant S^n, \tag{6.21}$$

where

$$S^n = \max\{|\, S_{pq}^n \,|\}_{p,q\in\{0,1\}}.$$

Thus, our version of the timesplitting scheme preserves $\sum_{(i,j)\in M_{pq}} \omega_{ij} = 0$ in an unconditionally stable manner.

## VII. A Brief Description of The Hybrid Scheme

To understand how the hybrid scheme works, one should think of the Navier–Stokes equations as they are written in (6.1), that is, in vorticity formulation. The key to this scheme is the dual treatment of vorticity. We have a vorticity field on the mesh and we have point vortices which are generated from the tangential components of the boundary forces as described in Section III. The point vortices are retained as point vortices for a specified number of timesteps, after which their vorticity is spread to the mesh and they are dropped from the calculation.

We now give a brief overview of the hybrid scheme, which will be detailed in the next section. At each timestep, the forces are updated, the oldest vortices are spread to the mesh and new ones are created in their place using the updated tangential forces. Then the normal forces are spread to the mesh and their discrete curl is taken. Next the mesh vorticity is updated using (6.5)–(6.6), which involve the curl of the normal forces, and the total velocity, which will be described below. We spread the vorticity of the point vortices to the mesh, obtaining the total vorticity field $\omega_{ij} + \tilde{\omega}_{ij}$, where $\omega_{ij}$ is the mesh vorticity and $\tilde{\omega}_{ij}$ is the field due to the point vortices. The stream function $\psi$ ought to satisfy

$$\Delta\psi = \omega + \tilde{\omega} \tag{7.1}$$

so we discretize this and solve

$$(D_{01}^2 + D_{02}^2)\,\psi^{n+1} = \omega^{n+1} + \tilde{\omega} \tag{7.2}$$

using the fast Laplace solver on the four meshes as described in Section VI. Note that we need to know that $\sum_{(i,j)\in M_{p,q}} \omega_{ij}^{n+1} = 0$. This is, in fact, true because of our method of spreading vorticity to the mesh and it will be proved below. The streamfunction $\psi^{n+1}$ is differenced as in (6.7) to obtain a velocity field $u$. Recall that in this particular example we are studying the filling cycle of the heart. We therefore need a source of volume to represent blood returning from the lungs. The velocity of a point source of constant strength is thus added to $u$ to obtain $u^{n+1}$, the total velocity. The velocity of, the point source is curl free so that $Cu^{n+1} = \omega^{n+1} = \omega^{n+1} + \tilde{\omega}$ is still true; however, the velocity is not divergence free at the source itself. As our final step, we move the boundary points and point vortices by interpolating $u^{n+1}$ to each of those points. The vortices are also walked one random step because of diffusion.

We now describe how the spreading of vorticity and force and the interpolation of velocity are accomplished. Let $\mathbf{x}_k = (x_{1k}, x_{2k})$ be the location of a point vortex (with strength $K_k$) or of a boundary point and let the mesh points be located at $\{(ih, jh)\colon 0 \leqslant i, j \leqslant 1/h\}$. Then the vorticity field due to the point vortices satisfies

$$\tilde{\omega}(x_1, x_2) = \sum_k K_k \delta(x_{1k} - ih)\,\delta(x_{2k} - jh), \tag{7.3}$$

where we have changed notation somewhat and $\delta$ is the one-dimensional Dirac $\delta$-function. The boundary force and the velocity satisfy the equations

$$\mathbf{F}(x_1, x_2) = \int_0^L \mathbf{f}(s)\, \delta(x_1 - X_1(s))\, \delta(x_2 - X_2(s))\, ds \tag{7.4}$$

and

$$\mathbf{u}(x_1, x_2) = \int_0^1 \int_0^1 \mathbf{u}(y_1, y_2)\, \delta(x_1 - y_1)\, \delta(x_2 - y_2)\, dy_2\, dy_1 . \tag{7.5}$$

We discretize (7.3)–(7.5) as follows.

$$\tilde{\omega}_{ij} = \sum_k K_k d(x_{1k} - ih)\, d(x_{2k} - jh), \tag{7.6}$$

$$\mathbf{F}_{ij} = \frac{1}{N} \sum_1^N \mathbf{f}_k d(x_{1k} - ih)\, d(x_{2k} - jh), \tag{7.7}$$

$$\mathbf{u}_k = h^2 \sum_{i,j} \mathbf{u}_{ij} d(x_{1k} - ih)\, d(x_{2k} - jh), \tag{7.8}$$

where

$$\begin{aligned} d(x) &= \frac{1}{4h}\left(1 + \cos\left(\frac{\pi x}{2h}\right)\right), && |x| < 2h, \\ &= 0, && |x| \geqslant 2h. \end{aligned} \tag{7.9}$$

This approximation to the one-dimensional Dirac $\delta$-function was introduced in Peskin [8]. Its many useful properties are discussed in that paper. Here we shall only need the following.

$$\sum_j hd(x - (2j + 1)h) = \sum_j hd(x - 2jh) = \tfrac{1}{2}. \tag{7.10}$$

Using (7.6) we see that

$$\begin{aligned} \sum_{(i,j)\in M_{pq}} \tilde{\omega}_{ij} &= \sum_k \sum_{(i,j)\in M_{pq}} K_k d(x_{1k} - ih)\, d(x_{2k} - jh) \\ &= \frac{1}{4h^2} \sum_k K_k \\ &= 0 \end{aligned} \tag{7.11}$$

because the vortices are created in dipole pairs of equal and poposite strength. This shows that $\tilde{\omega}$ falls in the range of our discrete Laplace operator on the periodic domain as required for the existence of the stream function.

## VIII. The Hybrid Scheme

We now detail the specifics of our hybrid scheme. Before doing so, we introduce some notation. Below. $\mathbf{X}_k$ is the location of a boundary point, $\mathbf{Y}_k$ that of a point vortex with strength $K_k$. There are $N$ of the former and $2NL$ of the latter, where $L$ is the number of timesteps for which vortices are retained. We have a pointer $P$, which is the index of the first of the oldest vortices. $\mathbf{f}_k$ will be the boundary force density and we have $\mathbf{f}_k = (f_\tau)_k\ \boldsymbol{\tau}_k + (f_n)_k\ \mathbf{n}_k$, where $\boldsymbol{\tau}$ and $\mathbf{n}$ are unit vectors parallel and perpendicular to the boundary, respectively. Letting $\mathbf{g}_k = f_{\tau k}\boldsymbol{\tau}_k$, we also define the quantity $C_k$ such that $C_k\mathbf{n}_k = (-g_{2,k}, g_{1,k})$. Note that we assume that the tangent and normal directions for our discretized boundary have already been defined.

The mesh quantities are $\mathbf{u}_{ij}$, the velocity; $\omega_{ij}$, the mesh vorticity; $\psi_{ij}$, the stream function; and $\mathbf{F}_{ij}$, the normal force. We also have a point source of strength $Q$, located at the point $(a, b)$. Finally, superscript $n$ indicates the $n$th timestep. A variable

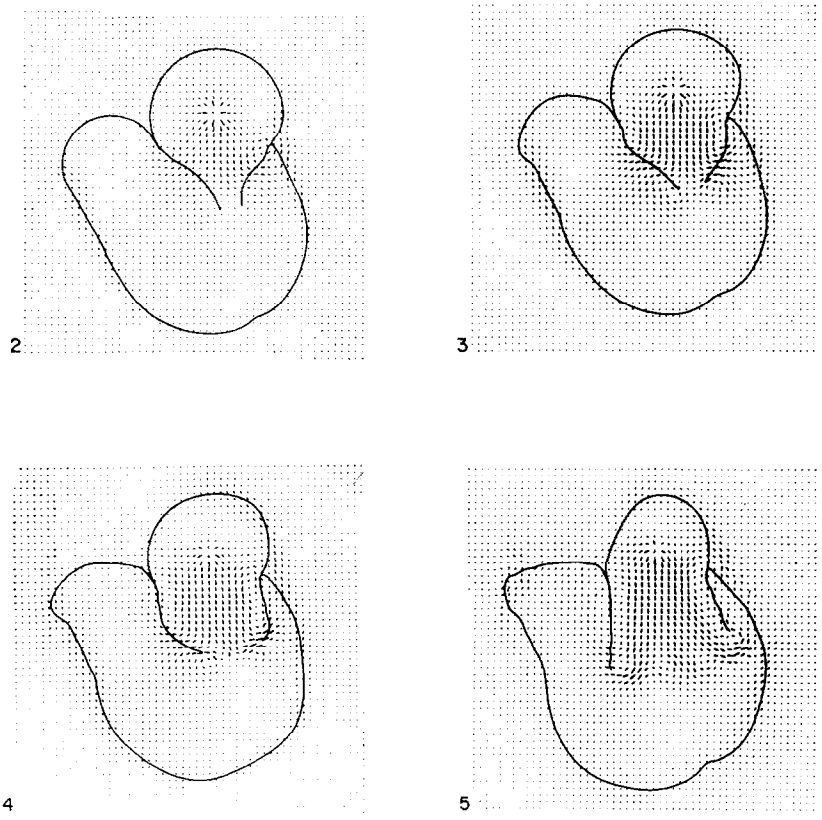


FIGS. 2–13. Frames from a run at $\frac{1}{10}$ the Reynolds number of the human heart.

FIGS 2–5. The opening of the valve.

with no superscript is an intermediate variable. The mesh width is $h$ and the timestep $\Delta t$.

The hybrid scheme is as follows. To find the forces, solve by Newton's method the nonlinear fixed-point problem

$$\mathbf{X}_k = [\mathbf{X}_k^n + \Delta t\, \mathbf{u}_k^n] + \lambda \mathbf{f}_k(\mathbf{X}_1, \ldots, \mathbf{X}_N)^4 \tag{8.1}$$

and evaluate the forces

$$\mathbf{f}_k^{n+1} = f_k(\mathbf{X}_1, \ldots, \mathbf{X}_N). \tag{8.2}$$

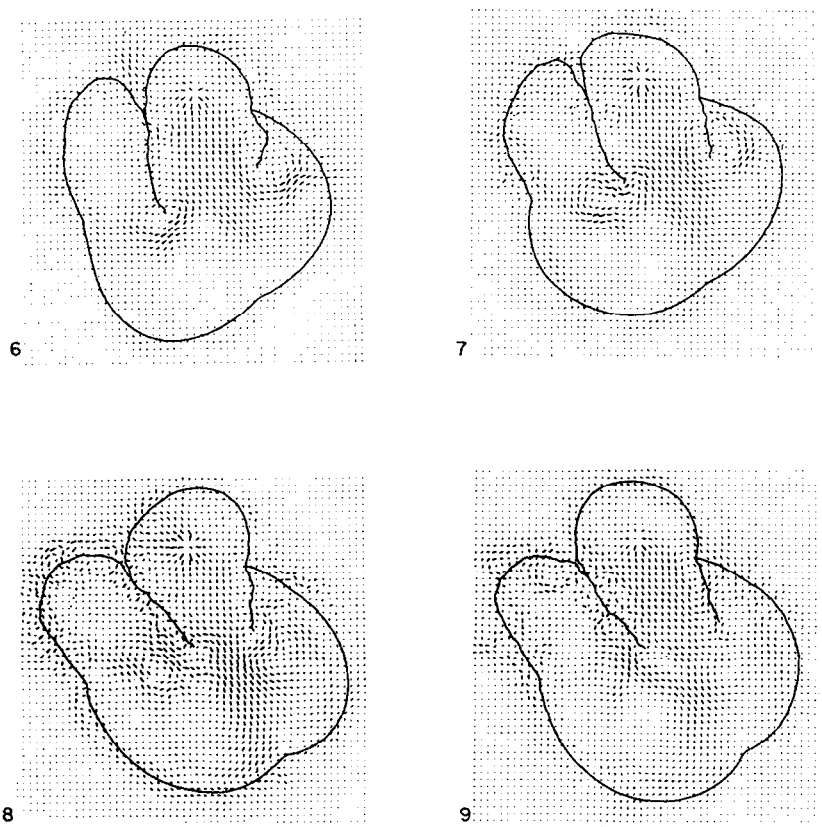


FIGS. 2–13—*Continued*

FIG. 6. Vortices form at the tips of the valve leaflets.
FIG. 7. The valve drifts toward closure under the influence of the vortices.
FIG. 8. The valve drifts toward closure.
FIG. 9. Atrial systole: the atrium contracts, opening the valve to squeeze out the last jet of blood.

[4] A complete discussion of this equation is given in Peskin [8]. One may choose $\lambda$ freely. It should be chosen to produce numerical stability.

Spread the oldest vortices to the mesh,

$$\omega_{ij}^n = \omega_{ij}^n + \sum_{k=P}^{P+2N-1} K_k d(Y_{1,k}^n - ih)\, d(Y_{2,k}^n - jh), \tag{8.3}$$

and create new vortices at the locations

$$\begin{aligned} \mathbf{Y}_{2j-1}^n &= \mathbf{X}_j^n + h\mathbf{n}_j, \\ \mathbf{Y}_{2j}^n &= \mathbf{X}_j^n - h\mathbf{n}_j, \qquad \text{for } \frac{P+1}{2} \leqslant j \leqslant \frac{P-1}{2} + N, \end{aligned} \tag{8.4}$$

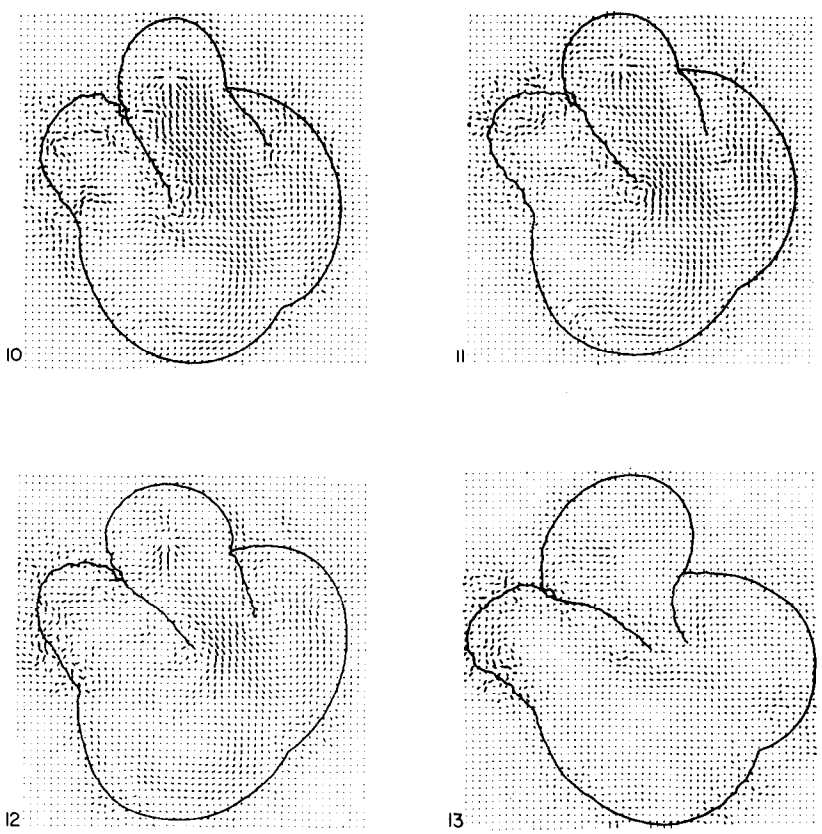


FIGS. 2–13—*Continued*

FIG. 11. Ventricular systole: the valve starts to close.
FIG. 13. The valve closes.

with the following strengths determined by the tangential forces:

$$K_{2j-1} = \frac{C_j \Delta t}{2hN},$$
$$K_{2j} = \frac{-C_j \Delta t}{2hN}, \qquad \frac{P+1}{2} \leqslant j \leqslant \frac{P-1}{2} + N. \tag{8.5}$$

Spread the normal forces to the mesh,

$$\mathbf{F}_{ij}^{n+1} = \frac{1}{N} \sum_{k=1}^{N} (f_n)_k \, \mathbf{n}_k d(X_{1,k} - ih) \, d(X_{2,k} - jh). \tag{8.6}$$

Update the mesh vorticity using the timesplitting method

$$\omega^{n+1/2} - \omega^n = \frac{\Delta t}{2}\left[-D_{01}(u_1{}^n \omega^{n+1/2}) - D_{02}(u_2{}^n \omega^n) + \frac{1}{R} D_{+1}D_{-1}\omega^{n+1/2} + \frac{1}{R} D_{+2}D_{-2}\omega^{n+1/2} + C\mathbf{F}^{n+1}\right], \tag{8.7}$$

$$\omega^{n+1} - \omega^n = \frac{\Delta t}{2}\left[-D_{01}(u_1{}^n \omega^{n+1/2}) - D_{02}(u_2{}^n \omega^{n+1}) + \frac{1}{R} D_{+1}D_{-1}\omega^{n+1/2} + \frac{1}{R} D_{+2}D_{-2}\omega^{n+1} - C\mathbf{F}^{n+1}\right].$$

Find the stream function,

$$((D_{01}^2 + D_{02}^2)\, \psi^{n+1})_{ij} = \omega_{ij}^{n+1} + \sum_{k=1}^{2LN} K_k d(X_{1,k} - ih) \, d(X_{2,k} - jh), \tag{8.8}$$

and the new velocity field,

$$u_1 = -D_{02}\psi^{n+1},$$
$$u_2 = D_{01}\psi^{n+1}; \tag{8.9}$$

$$\mathbf{S}_{ij} = \frac{Q}{2\pi} \frac{(ih - a, jh - b)}{(ih - a)^2 + (jh - b)^2}; \tag{8.10}$$

$$\mathbf{u}^{n+1} = \mathbf{u} + \mathbf{S}. \tag{8.11}$$

Evaluate the velocity at the boundary points,

$$\mathbf{u}_k^{n+1} = h^2 \sum_{i,j} \mathbf{u}_{ij}^{n+1} d(X_{1,k} - ih) \, d(X_{2,k} - jh), \tag{8.12}$$

and move the boundary points,

$$\mathbf{X}_k^{n+1} = \mathbf{X}_k{}^n + \Delta t \, \mathbf{u}_k^{n+1}. \tag{8.13}$$

Similarly, evaluate the velocity field at the vortices,

$$\mathbf{u}_l^{n+1} = h^2 \sum_{i,j} \mathbf{u}_{ij}^{n+1} d(Y_{1,l} - ih)\, d(Y_{2,l} - jh), \tag{8.14}$$

and move the vortices,

$$\mathbf{Y}_l^{n+1} = \mathbf{Y}_l^{n} + \Delta t\, \mathbf{u}_l^{n+1} + \boldsymbol{\eta}_l^{n+1}, \tag{8.15}$$

where $\mathbf{n}_l^n$ are independent, Gaussian random variable with mean zero and variance $\Delta t/R$.

## IX. Results and Conclusions

To study the flow patterns of the mitral valve, we use a square, 64 by 64 grid. The heart has about 300 boundary points. The filling part of the cardiac cycle takes about

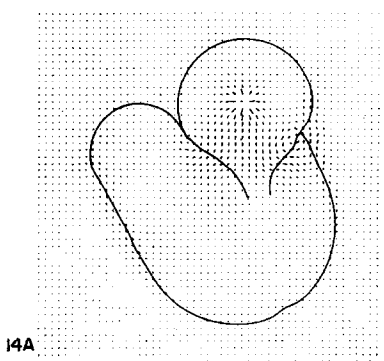


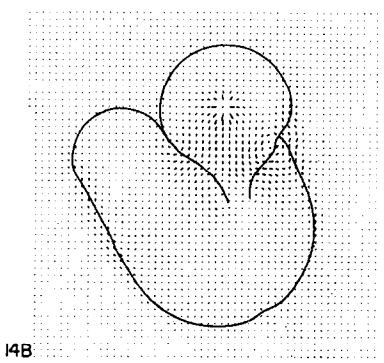


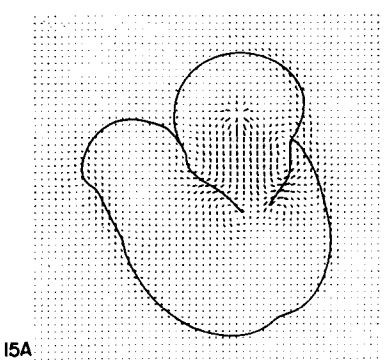


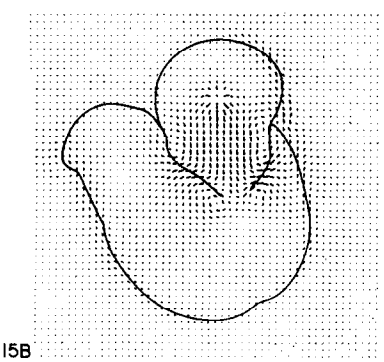


Figs. 14–19. Frames at different Reynolds numbers.

Figs. 14A, 15A. One-half the Reynolds number of the human heart.
Figs. 14B, 15B. The Reynolds number of the human heart.

600 timesteps. In the present work, vortices are retained for five time steps, the time step is 0.00035 and the source strength is 8. Our program uses $136{,}000_8$ words of core and about 2 hr CPU time to run on a CDC 6600. The output is in the form of plots. In Figs. 2–13, we have selected frames from a run at 0.1 times the Reynolds number of the human heart. Unfortunately, because of the very large forces generated at the boundary during ventricular systole, we are unable to complete the runs that we have made at higher Reynolds numbers. The boundary becomes unstable during ventricular systole, which is the event that terminates the filling cycle of the valve. We are working to eliminate this problem, Figures 14A–19A and 14B–19B show, respectively, frames from runs at $\frac{1}{2}$ the Reynolds number of the human heart and at the actual Reynolds number of the human heart. These frames are from the same stages in the cardiac cycle as those in Figs. 2–7. One can easily see that our method supports the conclusion that the natural mitral valve behaves independently of Reynolds number. This may

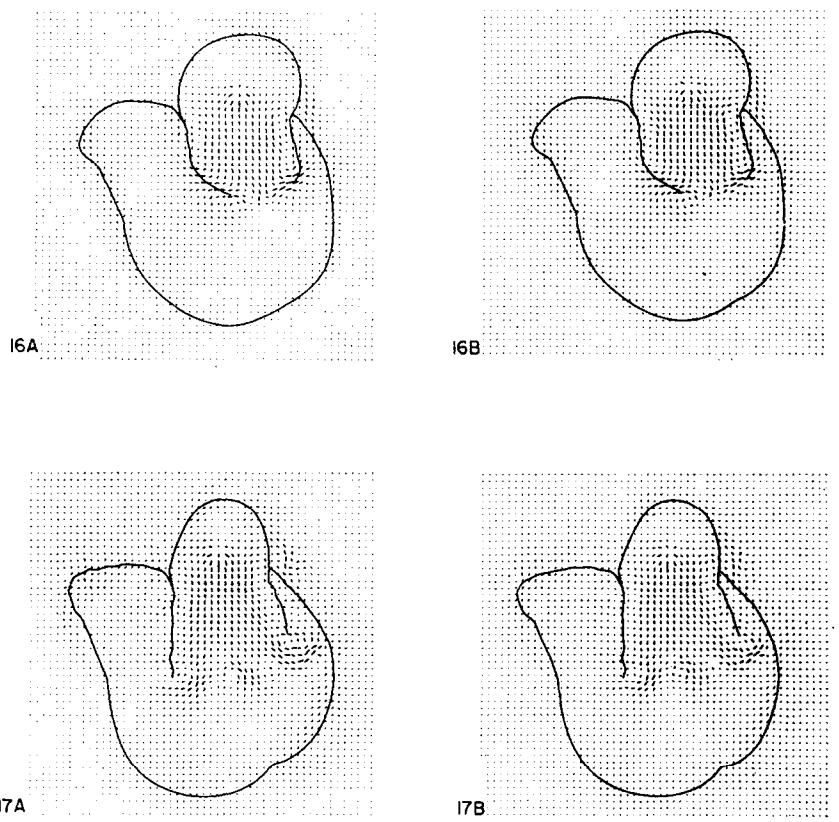


FIGS. 14–19—*Continued*

FIGS. 16A. 17A. One-half the Reynolds number of the human heart (contnued).
FIGS. 16B, 17B. The Reynolds number of the human heart (continued).

not be true of artificial valves and should be checked, since the Reynolds number [redacted] under clinically relevant conditions such as anemia (which gives low vis-

agree well with experiments, this supports the conclusion that our method is a good one. We do not yet know, however, whether the method will work as well on problems in which the solution has a strong dependence on the Reynolds number. This point is being checked now. We believe that our method is a good candidate for solving the incompressible Navier–Stokes equations in two dimensions at moderately high Reynolds numbers in the case of interior flows with complicated, moving boundaries whose motion is not known in advance. The work of computation does not increase with Reynolds number because the mesh does not have to be refined and the number of vortices does not need to increase. However, at very high Reynolds numbers, it

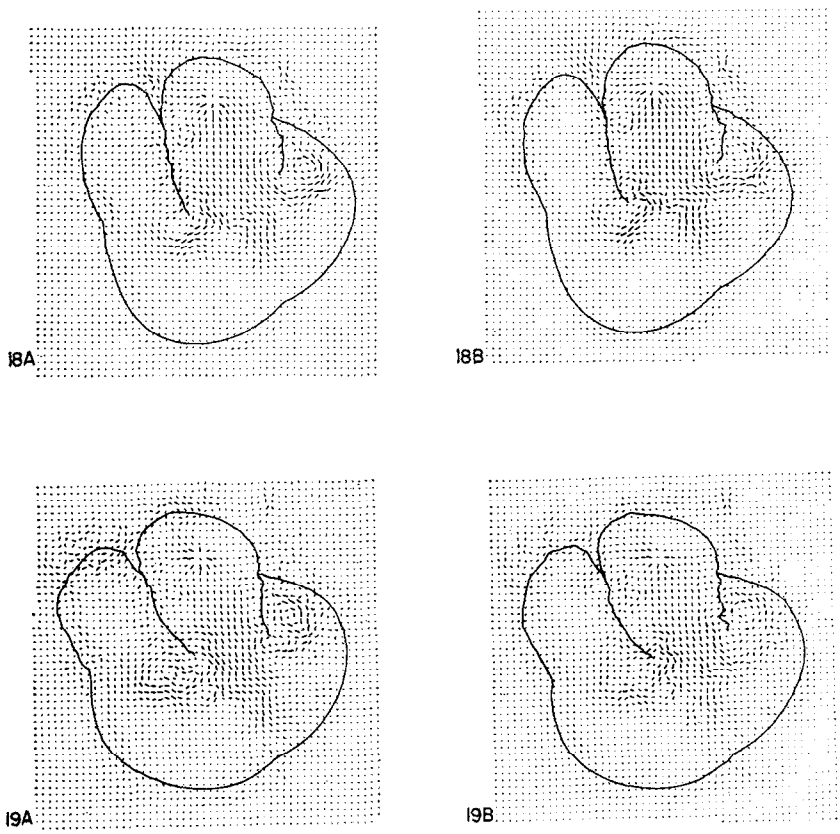


FIGS. 41–19—*Continued*

FIGS. 18A, 19A. One-half the Reynolds number of the human heart (continued).
FIGS. 18B, 19B. The Reynolds number of the human heart (continued).

would probably be best to introduce a local correction to the velocity field to make up for the smoothing effects of the mesh. This would, of course, increase the work of computation.

Finally, we remark that it would obviously be desirable to do a three-dimensional study of valve motion. Until recently, this could not be contemplated because of the lack of an appropriate high-Reynolds-number method. However, Buneman *et al.* [10] are developing a method which we may be able to use on this problem sometime in the future.

## ACKNOWLEDGMENTS

Many people have made useful suggestions and contributions to this work. The authors would particularly like to thank A. J. Chorin, D. McQueen, O. Widlund, and E. L. Yellin for interesting conversations; M. Brothers and D. McQueen for helping with the computing; and J. Race for the beautiful job she did typing the manuscript. The research was partially supported by the National Science Foundation under Grant NSF MCS-76-07039 and by the National Institutes of Health under Research Grant HL-17859. Computation was supported by Indiana University and by the U.S. Department of Energy under Contract EY-76-C-02-3077 at the Courant Mathematics and Computing Laboratory of New York University.

## REFERENCES

1. A. J. CHORIN, *in* "Proceedings, Third International Conference on Numerical Methods in Fluid Dynamics, Paris, 1972," pp. 100–104, Lecture Notes in Fluid Dynamics No. 19, Springer-Verlag, New York/Berlin, 1973.
2. T. E. DUSHANE, *Math. Comput.* **27** (1973), 124.
3. FISCHER, GOLUB, HALD, LEIVA, AND WIDLUND, *J. Math. Comput.* **28** (1974), 126.
4. O. HALD, preprint.
5. D. KALMANSON (Ed.), "The Mitral Valve," Publishing Sciences Group, Acton, Mass., 1976.
6. R. MENDEZ, Thesis, University of California, Berkeley, 1978.
7. C. S. PESKIN, "Mathematical Aspects of Heart Physiology," Courant Institute of Mathematical Sciences (New York University), Lecture Notes, 1975.
8. C. S. PESKIN, *J. Comput. Phys.* **25** (1977), 3.
9. A. I. SHESTAKOV, "Numerical Solution of the Navier–Stokes Equations at High Reynolds Numbers," National Technical Information Service, U.S. Dept. of Commerce, UCRL 51894.
10. O. BUNEMAN, B. COUËT, AND A. LEONARD, *in* "Proceedings, Sixth International Conference on Numerical Methods in Fluid Dynamics," Springer-Verlag, New York/Berlin, in press.
11. M. F. MCCRACKEN AND C. S. PESKIN, *in* "Proceedings, Sixth International Conf. on Numerical Methods in Fluid Dynamics, 1978," Springer–Verlag, New York/Berlin, in press.